Bragg solitons in nonlocal nonlinear media

YuanYao Lin,[1] Ray-Kuang Lee,[1] and Boris A. Malomed[2]
[1]*Institute of Photonics Technologies, National Tsing-Hua University, Hsinchu 300, Taiwan*
[2]*Department of Physical Electronics, School of Electrical Engineering, Faculty of Engineering, Tel Aviv University, Tel Aviv 69978, Israel*
(Received 5 May 2009; published 31 July 2009)

We derive nonlocal coupled-mode equations for a Bragg grating embedded in a medium with nonlocal nonlinearity. Using these equations, we study the oscillatory instability of nonlocal Bragg solitary waves and demonstrate that collisions between them result in fusion into a standing pulse (or breather), possibly with generation of additional jets, in a broad range of parameters. The results are explained by considering the effect of spatial dispersion induced by the nonlocal nonlinear response.

DOI: 10.1103/PhysRevA.80.013838 PACS number(s): 42.65.Tg, 42.65.Sf, 42.70.Qs

I. INTRODUCTION

Photonic crystals (PhCs) have become a ubiquitous concept in modern optical physics and engineering. Using the Bragg reflections, one can engineer desirable modifications of dispersion relations for the transmission of light in PhC media. In particular, the group velocity can be controlled by detuning the wave from the exact Bragg resonance [1]. With the properly designed dispersion at relevant wavelengths, PhCs provide unique possibilities for the implementation of optical sensing [2], photonic circuits [3], optical signal processing, and optical computation networks [4,5]. As a result of the interplay of the material Kerr nonlinearity and the band-gap spectrum of the PhC, robust gap solitons or, more generally speaking, Bragg solitary waves (BSWs) can be formed in the band gap, as was predicted theoretically [6,7] and demonstrated experimentally in optical fibers with the grating written in the cladding [8]. On a par with the temporal BSWs, spatial Bragg solitons were predicted too in Kerr-nonlinear planar waveguides equipped with a spatial grating [9,10].

Combining the benefits of PhC modes and ordinary solitons, the BSWs have a great potential for fundamental and applied studies in photonics. The stability of BSW families against oscillatory perturbations [11–13] and the related modulational instability [14] have been studied in detail. BSWs in supergratings [15–21] and the mobility of solitons in lattice potentials [22], as well as collisions between solitons in the standard model [23] and in generalized ones, with the cubic-quintic nonlinearity [24] or dispersive reflectivity [25], have been studied too. BSWs have drawn special attention due to their ability to generate slow-light solitons in apodized [26–28] and chirped [20] gratings, as well as by decelerating the pulses by way of collisions between them [23,25].

It is also known that nonlocal nonlinearity helps to suppress symmetry-breaking instabilities of solitons when the correlation radius of the dielectric response becomes comparable to the transverse size of the soliton [29,30]. In the presence of the nonlocality, interactions between solitons vary broadly due to the action of long-ranged forces [31]. An example of such nonlocal media is a nematic liquid crystal with tunable nonlocality, which results from the control of the molecular orientation by the external electrical field [32]. Regarding gap solitons, nonlocal nonlinearity may stabilize them against the modulational instability due to reduction in the effective nonlinearity [33,34], and enhance their mobility, which may be explained by the diminution of the Peierls-Nabarro (PN) potential barrier in PhC [33,34].

In this work, we first aim to derive nonlocal coupled-mode (CM) equations, following the general procedure of the derivation of the Bragg model equations in the spatial domain, from nonlinear Schrödinger equations governing the wave transmission in a one-dimensional PhC with the shallow modulation of the refractive index and nonlocal nonlinearity, which is done in Sec. II. Then, in Sec. III we investigate oscillatory instabilities of a numerically found family of BSWs in nonlocal nonlinear media with a generic nonlocal response of the diffusion type. In Sec. IV we study collisions of counter-propagating BSWs in the medium of this type. A parameter region in which two colliding BSWs merge into a standing wave is identified, turning out to be much larger than in the standard model [23]. We explain the significantly enhanced interaction between BSWs in this nonlocal medium in terms of its effective spatial dispersion. The results clearly suggest that the nonlocal nonlinear response can suppress oscillatory instabilities in BSWs, and that a weak nonlocal nonlinearity offers a promising way to generate slow-light solitons via collision between BSWs.

II. DERIVATION OF NONLOCAL COUPLED-MODE EQUATIONS

To derive the nonlocal version of CM equations, we start with the usual nonlocal model in the spatial domain, which includes a periodic potential representing the grating. In the normalized form with dimensionless coordinates, the equations are

$$i\phi_z = -\frac{1}{2}\phi_{xx} + [n - \epsilon\cos(Gx)]\phi,$$

$$n - dn_{xx} = |\phi|^2, \tag{1}$$

where ϕ is the local amplitude of the electromagnetic wave, z the propagation distance, x the transverse coordinate, and

$n(x,z)$ a local perturbation of the refractive index induced by the nonlocal response. Coefficient d determines the correlation length, $\sim 1/\sqrt{d}$, of the respective nonlocal kernel, while G and ϵ are the wavenumber and strength of the grating, respectively.

To derive the CM equations from Eqs. (1), we assume, as usual, that in the first band gap the solution to the nonlocal equations is represented by a superposition of two counterpropagating wave packets [35],

$$\phi(x,z) = \frac{\sqrt{\epsilon}}{2}[U(x,z)\exp(iGx/2) + V(x,z)\exp(-iGx/2)], \tag{2}$$

and substitute it into Eq. (1). Keeping only first derivative of the slowly varying amplitudes, we obtain

$$i\frac{\partial U}{\partial z} + i\frac{G}{2}\frac{\partial U}{\partial x} - \left(\frac{G}{2}\right)^2 U - \left|\frac{\epsilon}{4}\right|(n_0 U + n_1 e^{-iGx}V) + \frac{\epsilon}{2}V = 0, \tag{3}$$

$$i\frac{\partial V}{\partial z} - i\frac{G}{2}\frac{\partial V}{\partial x} - \left(\frac{G}{2}\right)^2 V - \left|\frac{\epsilon}{4}\right|(n_0 V + n_1^* e^{iGx}U) + \frac{\epsilon}{2}U = 0, \tag{4}$$

$$n_0 - d\frac{d^2 n_0}{dx^2} = |U|^2 + |V|^2, \tag{5}$$

$$n_1 - d\frac{d^2 n_1}{dx^2} = UV^* e^{iGx}, \tag{6}$$

where n_0 is the slowly varying part of the local perturbation of the refractive index. Assuming that the bandwidth of Fourier transforms of functions U and V is much smaller than G, Eq. (6) can be easily solved by means of the Fourier transform, $n_1 \approx (1+dG^2)^{-1}UV^* \exp(iG\xi)$, or more explicitly

$$\hat{n}_1 = \frac{\hat{U} \otimes \hat{V}^* \otimes \delta(k_x - G)}{1 + dk_x^2}, \tag{7}$$

where $\otimes$ stands for the convolution and $\hat{n}_1$, $\hat{U}$, and $\hat{V}$ are the Fourier transforms of n_1, U, and V, respectively. Making use of this approximation, one can readily derive the CM equations for the nonlocal medium in the final form

$$i\frac{\partial U}{\partial \eta} + i\frac{\partial U}{\partial \xi} - \frac{1}{2}\left[n_0 + \frac{|V|^2}{1+Dg^2}\right]U + V = 0, \tag{8}$$

$$i\frac{\partial U}{\partial \eta} - i\frac{\partial V}{\partial \xi} - \frac{1}{2}\left[n_0 + \frac{|U|^2}{1+Dg^2}\right]V + U = 0, \tag{9}$$

$$n_0 - D\frac{\partial^2 n_0}{\partial \xi^2} = |U|^2 + |V|^2, \tag{10}$$

where n_0 is the slowly varying part of the local perturbation of the refractive index, and $\eta \equiv \epsilon z/2$, $\xi \equiv \epsilon x/G$, $D \equiv d\epsilon^2/G^2$, and $g \equiv G^2/\epsilon$. Starting with the wave equation incorporating the instantaneous nonlocal response, instead of Eq. (1), one will end up with a counterpart of the CM system in Eqs. (8)–(10) in the temporal domain, with η being the scaled temporal variable. In the latter case, the model is valid provided that it describes the nonlinear evolution which is much slower than the relaxation of the nonlocal changes in the refractive index. In the limit of the local response, the latter model can be reduced to the standard system of local CM equations in the Kerr medium, with the ratio of the (self/cross-)phase-modulation coefficients equal to 1/2 [6,7].

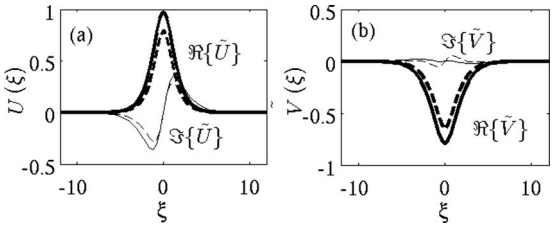

FIG. 1. In panels (a) and (b), the plots of real and imaginary parts of fields $\tilde{U}(\xi)$ and $\tilde{V}(\xi)$ (denoted by the respective Gothic symbols) represent generic examples of the Bragg solitons in the local and nonlocal models, respectively, with $D=0.5$, $\theta=0.3$, and $v=0.2$. The solid and dashed curves show, respectively, the real and imaginary parts of $\tilde{U}(\xi)$ and $\tilde{V}(\xi)$.

BSWs residing in the first Bragg band gap—generally speaking, with spatial tilt or velocity v—can be looked for as $\{U(\xi;\eta), V(\xi,\eta)\} = \{\tilde{U}(\xi), \tilde{V}(\xi)\}\exp(iq\eta)$. In the linear approximation, Eq. (10) decouples from Eqs. (8) and (9). The linearization of the two latter equations give rise to the same band gap and constraint on the spatial tilt (velocity) of oblique (moving) modes as the standard CM system, i.e., severally, $q^2<1$ and $v^2<1$. Thus, the propagation constant for BSWs may be chosen in the same form as in standard solutions [6,7], $q=\cos\theta$, which covers the whole gap while parameter θ varies in interval $0<\theta<\pi$. Thus, one may parameterize the entire soliton family by the pair of θ and v.

The BSW family was constructed as a numerical solution to Eqs. (8)–(10) with boundary conditions $\tilde{U}(\pm\infty)$, $\tilde{V}(\pm\infty)=0$. The results may be adequately represented by fixing $g=4$ in Eqs. (8)–(10). Examples of the corresponding local and nonlocal solutions are displayed, respectively, by solid and dashed lines in Figs. 1(a) and 1(b), for $D=0.5$, $\theta=0.3$, and $v=0.2$. The boldfaced and lightfaced curves show the real and imaginary parts of $\tilde{U}(\xi)$ and $\tilde{V}(\xi)$. The entire family of the nonlocal Bragg solitons is represented in Fig. 2 by means of the curve showing the total power,

$$Q \equiv \int_{-\infty}^{\infty} |U(\xi)|^2 + |V(\xi)|^2 d\xi, \tag{11}$$

versus parameter $\theta \equiv \arccos q$. In the presence of the nonlocality, the power necessary for the formation of BSWs increases against their counterparts in the local medium, similar to the situation known in other nonlocal models [29–34].

The nonlocal response function employed in the above analysis is assumed to correspond to a steady state, with the duration of the nonlinear interaction much longer than the time scale of the diffusional relaxation of perturbations of the

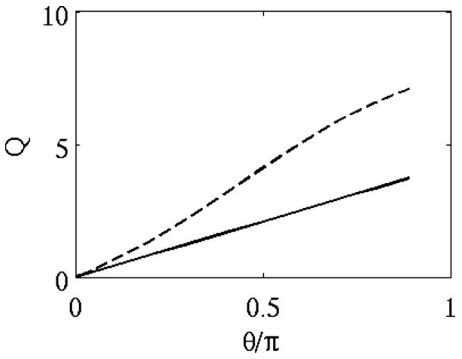

FIG. 2. The total power, Q, of the Bragg solitons in local (solid) and nonlocal (dashed) media versus the intrinsic parameter, θ, which is determined by the propagation constant, $q=\cos\theta$, for nonlocality $D=0.5$, and $v=0$.

refractive index. Real optical media to which this nonlocal model applies are photorefractive crystals [37,38], whose nonlocal nonlinearity results from the photovoltaic effect and diffusion-driven charge transport with a typical response time on the order of hundreds nanoseconds [39]. In other media—for instance, liquid crystals [40–42], thermal-optical materials [43,44], and even plasmas [45]—direct observation of nonlocal nonlinearities of the diffusion type was also reported.

III. OSCILLATORY INSTABILITY OF THE BRAGG SOLITONS

Oscillatory instabilities is a well-known property of multicomponent solitons, which ensues from a collision of two originally stable eigenvalues of small-perturbation modes [12,14]. In the model of the local medium, the oscillatory instability was found within the framework of the standard CM system [11,12,36]. However, the analysis of this instability, based on either the Fourier decomposition or a finite-difference scheme, was reported to provide poor accuracy and spurious eigenvalues [11,36,46]. Therefore, for the BSWs in the present nonlocal model, we study the oscillatory instability by finding zeros of the Evans function in the wedge space [47,48], using the linearization of the CM equations.

First, solutions are substituted into the CM equations in an explicitly complex form, $\tilde{U}=R_1+iP_1$,$\tilde{V}=R_2+iP_2$, which converts Eqs. (8) and (9) into a matrix equation,

$$\left[\mathbf{M}\frac{\partial}{\partial\eta}+\mathbf{K}\frac{\partial}{\partial\xi}-\mathbf{J}-\frac{1}{2}n_0\mathbf{I}\right]Y_0=\frac{1}{2(1+Dg^2)}\begin{pmatrix}\sigma_g & 0\\ 0 & \sigma_g\end{pmatrix}Y_0, \tag{12}$$

where $Y_0(\xi,\eta)\equiv[R_1,R_2,P_1,P_2]^{\mathrm{T}}$, the matrices are defined as

$$\mathbf{M}=\begin{pmatrix}0 & \sigma_0\\ -\sigma_0 & 0\end{pmatrix},\quad \mathbf{K}=\begin{pmatrix}0 & \sigma_3\\ -\sigma_3 & 0\end{pmatrix},$$

$$\mathbf{I}=\begin{pmatrix}\sigma_0 & 0\\ 0 & \sigma_0\end{pmatrix},\quad \mathbf{J}=\begin{pmatrix}\sigma_1 & 0\\ 0 & \sigma_1\end{pmatrix}, \tag{13}$$

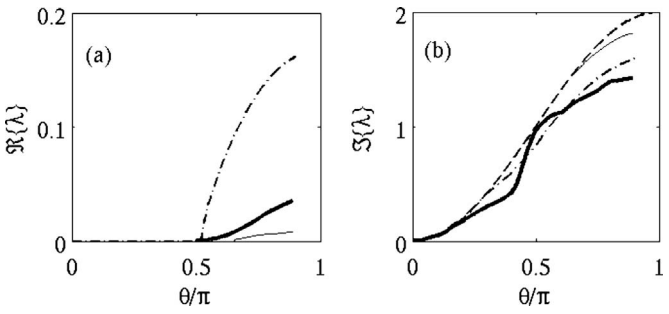

FIG. 3. The oscillatory instability of the Bragg solitons with zero velocity. Real (a) and imaginary (b) parts of the eigenvalues represent unstable perturbations in the local Kerr medium (dashed-dotted lines), and two branches of the instability (boldfaced and lightfaced solid lines) in the nonlocal nonlinear medium. Dashed lines in (b) refer to the imaginary part of the (stable) eigenvalues for solitons in the integrable massive Thirring model, see the text.

$$\sigma_g=\begin{pmatrix}P_2^2+R_2^2 & 0\\ 0 & P_1^2+R_1^2\end{pmatrix}, \tag{14}$$

σ_0, σ_1, and σ_3 being the standard Pauli matrices.

Looking for eigenmodes of small perturbations corresponding to instability eigenvalues λ as

$$\hat{Y}(\xi,\eta)=(\hat{Y}_0(\xi)+\hat{y}(\xi)e^{\lambda\eta})e^{iq\eta}, \tag{15}$$

the linearization of Eq. (12) is rewritten as

$$\frac{d}{d\xi}\hat{y}=[\mathbf{A}_{\mathrm{local}}(\xi,\lambda)+\mathbf{A}_{\mathrm{nonlocal}}(\xi,\lambda,\hat{y})]\hat{y}, \tag{16}$$

with $\mathbf{A}_{\mathrm{local}}(\xi,\lambda)\equiv\mathbf{K}^{-1}[\mathbf{S}(\hat{y})+q\mathbf{I}-\lambda\mathbf{M}]$ and

$$\mathbf{S}(\hat{y})=\frac{1}{2(1+Dg^2)}\begin{pmatrix}\sigma_g & \sigma_h\\ \sigma_h & \sigma_g\end{pmatrix}+\frac{1}{2}n_0\mathbf{I}+\mathbf{J}+\frac{1}{1+Dg^2}\begin{pmatrix}R_1R_2\sigma_1 & \sigma_h\\ \sigma_h & P_1P_2\sigma_1\end{pmatrix}, \tag{17}$$

$$\sigma_h\equiv\begin{pmatrix}0 & P_2R_1\\ P_1R_2 & 0\end{pmatrix}. \tag{18}$$

As for the nonlocal part, it can be written using the convolution with the response function, $R(\xi)=(2D)^{-1/2}e^{-|\xi|/D}$, which corresponds to the second equation in system (1). Thus, four elements of the vector corresponding to the nonlocal term in Eq. (16) are cast in the following form ($l=1,2,3,4$):

$$[\mathbf{A}_{\mathrm{nonlocal}}(\xi,\lambda,\hat{y})\hat{y}]_l=\sum_{k=1,2,3,4}Y_{0l}(\xi)\times\int_{-\infty}^{\infty}\hat{y}_k(\xi')Y_{0k}(\xi')R(\xi-\xi')d\xi', \tag{19}$$

Although the use of the Evans function for nonlocal equations has been proposed for the study of master mode-locking equations in a model of a solid-state laser cavity, including nonlocal terms [49], the numerical implementation

of the method may encounter difficulties in the sense that the unnormalized Evans function vanishes for small eigenvalues and diverges for large ones. To avoid these problems, we here construct the Evans function in the wedge space, $\Lambda^2(\mathbf{C}^4)$, and utilize the normalization process proposed in Ref. [48]. Accordingly, the nonlocality is replaced by a projection function, $P(\xi)$, such that the last term in Eq. (16) becomes local with matrix $[\mathbf{A}_{\text{nonlocal}}(\xi,\lambda)]_{k,l}=P(\xi)Y_{0k}(\xi)Y_{0l}(\xi)$. Then, the evolutions equation in the wedge space can be written as

$$\frac{d}{d\xi}W=\mathbf{A}^{(2)}W, \tag{20}$$

with initial conditions given by an asymptotic solution to the eigenvalue problem based on Eq. (16),

$$W(\pm\infty)=\{F_p^{\pm}F_m^{\pm},F_p^{\pm},i\ \text{sgn}(q)(F_m^{\pm}-F_p^{\pm}),i\ \text{sgn}(q)(F_m^{\pm}-F_p^{\pm}),-2,F_p^{\pm}+F_m^{\pm}\}^{\text{T}}, \tag{21}$$

with

$$F_m^{\pm}\equiv\lambda\mp\sqrt{(\lambda-i|q|)^2+1}-i|q|$$

and

$$F_m^{\pm}\equiv\lambda\mp\sqrt{(\lambda+i|q|)^2+1}+i|q|,$$

where subscripts p and m denote the largest positive and negative eigenvalues from the spectrum of Eq. (16). The operator in wedge space $\Lambda^2(\mathbf{C}^4)$, which appears in Eq. (20), is

$$\mathbf{A}^{(2)}\equiv\begin{pmatrix} a_{11}+a_{22} & a_{23} & a_{24} & -a_{13} & -a_{14} & 0 \\ a_{32} & a_{11}+a_{33} & a_{34} & a_{12} & 0 & -a_{14} \\ a_{42} & a_{43} & a_{11}+a_{44} & 0 & a_{12} & a_{13} \\ -a_{31} & a_{21} & 0 & a_{22}+a_{33} & a_{34} & -a_{24} \\ -a_{41} & 0 & a_{21} & a_{43} & a_{22}+a_{44} & a_{23} \\ 0 & -a_{41} & a_{31} & -a_{42} & a_{32} & a_{33}+a_{44} \end{pmatrix}, \tag{22}$$

where a_{kl} are elements of $\mathbf{A}_{\text{local}}(\xi,\lambda)+\mathbf{A}_{\text{nonlocal}}(\xi,\lambda)$.

Since the trace, $\text{Tr}\{\mathbf{A}_{\text{local}}+\mathbf{A}_{\text{nonlocal}}\}$, is zero, the Evans function can be defined and constructed as the wedge product of two limit forms of a solution to Eq. (20) [47,48],

$$E(\lambda)\equiv W(\xi\to 0^+)\Lambda W(\xi\to 0^-)=\sum_{k=1}^{6}\sum_{l=1}^{6}W(\xi\to 0^+)_k W(\xi\to 0^-)_l\Sigma_{lk}, \tag{23}$$

where $\Sigma_{16}=\Sigma_{34}=\Sigma_{43}=\Sigma_{61}=1$, $\Sigma_{25}=\Sigma_{52}=-1$, and $\Sigma_{lk}=0$ otherwise.

Eigenvalues λ are points at which the Evans function vanishes. The nonlocal projecting function, $P(\xi)$, is found by numerically iterating the evolution in Eq. (20) until it converges. The eventual results are plotted in Fig. 3, for the oscillatory instability of BSWs with the zero velocity ($v=0$) in the local and nonlocal models, the latter one taken with $D=0.5$. For the local system, the results displayed in Figs. 3(a) and 3(b) are tantamount to those previously reported in Refs. [11,12,36]. Although the threshold value for the onset of the instability in the nonlocal BSWs, $\theta_{\text{th}}\approx 0.52$, is close to its counterpart in the local model [11], it is worthy to note that the moderate nonlocality ($D=0.5$) reduces the growth rate of the oscillatory instability [see the boldfaced line in Fig. 3(a)] roughly by 60%, cf. the dashed-dotted line in the same figure. This stabilization may be interpreted as resulting from the effective attenuation of the nonlinearity in the nonlocal system [29,34]. Another noteworthy feature revealed by the stability analysis for the BSWs in the nonlocal medium is the second (weaker) instability branch [the light-faced curve in Fig. 3(a)], which bifurcates from the stable spectrum at $\theta=0.67\pi$.

A well-known fact is that the local version of Eqs. (8) and (9) goes over into the integrable massive Thirring model (MTM) if the self-modulation term is dropped in the equations [in terms of Eqs. (8) and (9), this simply means dropping n_0]. In the framework of the MTM, all solitons are stable. In fact, the calculation of the respective eigenvalue, defined as in Eq. (15), yields it in a purely imaginary form, $\lambda_{\text{MTM}}=i(1-\cos\theta)$ [50,51]. It may be interesting to compare imaginary parts of the eigenvalues in the nonlocal and local versions of the present model with λ_{MTM}, which is shown by the dashed line in Fig. 3(b). One can observe that, at $\theta<0.6\pi$, the deviation of $\text{Im}\{\lambda\}$ of the first oscillatory-instability branch from λ_{MTM} is stronger in the local nonlinear medium (the dashed-dotted line) than in the nonlocal model, which corresponds to the boldfaced solid line in Fig. 3(b)—particularly, in the instability region, $\theta>0.52\pi$—which is also related to the fact that the instability of the local BSW is stronger.

IV. COLLISION OF BRAGG SOLITONS IN THE NONLOCAL MEDIUM

Different outcomes which are possible as results of collisions between BSW can be identified as elastic passage,

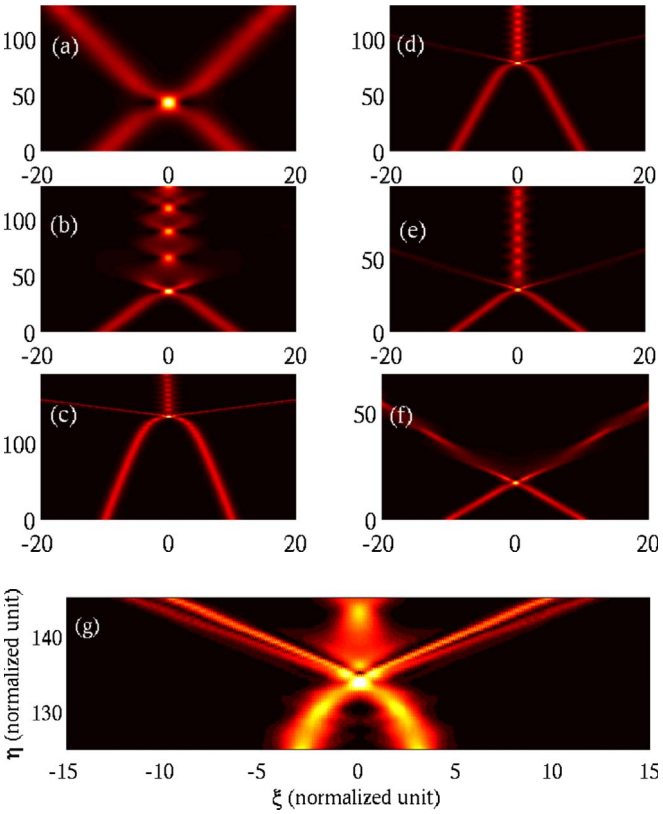

FIG. 4. (Color online) Typical examples of collisions between solitons in Eq. (10) with $D=0.5$, for the following sets of soliton parameters (θ,v): (a) $(0.14\pi, 0.1)$, (b) $(0.25\pi, 0.1)$, (c) $(0.85\pi, 0.1)$, (d) $(0.5\pi, 0.1)$, (e) $(0.5\pi, 0.3)$, and (f) $(0.5\pi, 0.5)$, which correspond to points A, B, C, D, E, F, and G in Fig. 6. Panel (g) is the enlargement of (c).

merger, symmetry breaking, and destruction, depending on velocities, amplitudes, and the relative phase of colliding solitons [23,25]. In this section, we consider the basic situation of the two BSWs with the opposite speeds and equal amplitudes and phases, to highlight new effect induced by the nonlocality.

Generic examples of the collisions are displayed in Fig. 4, for moderately strong effective nonlocality, $D=0.5$. At small amplitudes, the collisions are elastic [see Fig. 4(a)]. Above a certain amplitude threshold, the pair of BSWs merges into a single beam with zero velocity and conspicuous intrinsic vibrations, as shown in Fig. 4(b). The collisions between BSWs which are taken close to the upper edge of the band gap gives rise to *splitting*, i.e., the formation of a breather beam with zero velocity, and pairs of radiation beams ejected at very large transverse velocities, as seen in Fig. 4(c). The enlargement in panel Fig. 4(g) reveals that the radiation is actually emitted in the form of two transverse pairs of beams.

The mechanism underlying the splitting may be interpreted as an effective spatial dispersion, which stems from the nonlocal response of the medium. It can be estimated by term $D[\partial^2(|U|^2+|V|^2)/\partial\xi^2]$ in the asymptotic expansion of the nonlocal refractive index [30]. In the collision region, the nonlinear interference of the two solitons produces a strongly localized beam with a wide spectrum of spatial modes. As a result, waves propagating at different transverse velocities

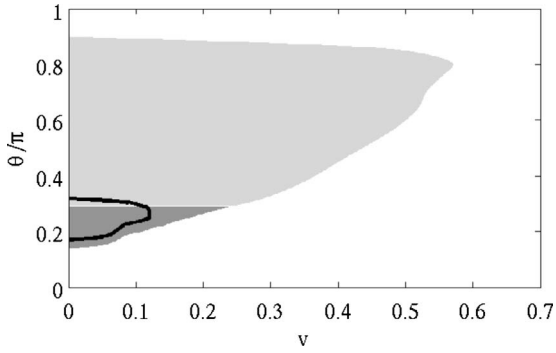

FIG. 5. Regions of the merger (M, dark gray) and merger with splitting (MS, light gray) for colliding Bragg solitons in the local and nonlocal media, with $D=0$ (enclosed within bold line) and $D=1$, respectively.

tend to separate from the beam. Although without the spatial dispersion in the local nonlinearity, very weak radiation jets can also be observed, for moving solitons with a large amplitude, outside the merger region in Fig. 5 – for example, at $\theta=0.35\pi$, $v=0.05$—the merge with splitting is indeed specific to nonlocal nonlinear media with the spatial dispersion. In other words, the nonlocality-induced spatial dispersion can suppress the PN potential barrier and enhance the wave's mobility [25,34,52,53], allowing radiation jet to escape. Simultaneously, this is a mechanism for dumping excess energy in the course of the collision. The possibility to eject the radiation jets facilitates the formation of merged standing-light solitons, as a result of the collision between moving BSWs. In Figs. 4(d)–4(f), which display the collisions with a fixed propagation constant but different velocities, one can also observe that, under the action of the spatial dispersion, the central fused beam becomes weaker, while the outward jets get stronger with the increase in the collision velocity.

In Fig. 5 we outline regions in the parameter space where the collisions between BSWs in the local and nonlocal model lead to the merger—region M—or a related outcome, the merger accompanied by the emission of transverse jets, in region MS (merger and splitting). For the standard local CM system, Fig. 5 shows that the merger is confined to a small range of $0.17\pi<\theta<0.32\pi$, at small values of collision velocity v (the area inside the bold line) [23]. With the introduction of the nonlocality, the shaded area in Fig. 5 demonstrates, at $D=1$, an abrupt expansion of the combined merger region (M and MS) to $0.14\pi<\theta<0.9\pi$, $v<0.6$. This effect is explained by the long-range attraction between wave components in the nonlocal medium, while the partial splitting in region MS is an effect of the enhanced spatial dispersion.

For a weaker nonlocality, e.g., $D=0.5$, the combined merger area is still much larger than its counterpart in the local model, as seen in Fig. 6. A notable feature, represented by the intrinsic white area in the latter panel, is that, in the region of $0.64\pi\lesssim\theta\lesssim0.8\pi$, the colliding BSWs fail to merge into a stable beam, completely splitting into multiple jets. In the case of $D=1$ (Fig. 5), this region disappears because the attractive interaction overwhelms the spatial dispersion. Figure 7 illustrates that more power is carried away by the radiation jets as the collision velocity increases. On the other

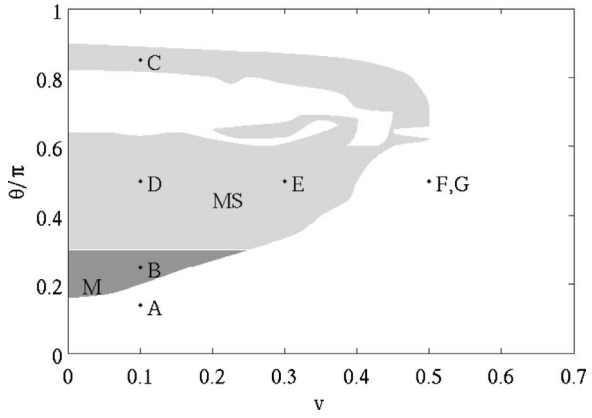

FIG. 6. Regions of the merger (M, dark gray) and merger with splitting (MS, light gray) for colliding Bragg solitons in the nonlocal medium with $D=0.5$

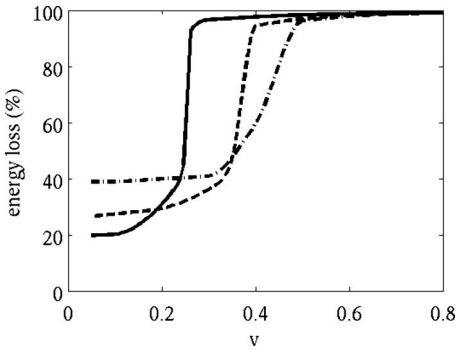

FIG. 7. The power share carried away by radiation jets at $D=0.5$, for $\theta=0.3$, 0.4, and 0.5 (solid, dashed, and dashed-dotted curves, respectively).

hand, for solitons with higher energy, the central fused beam retains a bigger power share at large transverse velocities ($v>0.3$), due to the strong long-range attraction.

In addition to the data displayed in Figs. 5–7, it is relevant to mention that the minimum integral power required to form the merged beam [see Eq. (11)] was found to be $Q_{\min}=1.4214$, 2.1125, and 2.1209 for $D=0$, 0.5, and 1, respectively. The increase of $Q_{\min}$ with the strength of the nonlocality is explained by the fact that one needs a higher power to overcome the above-mentioned spatial dispersion [32].

V. CONCLUSION

In this work, we have derived the CM equations for the Bragg grating embedded in a nonlocal nonlinear medium. Within the framework of these equations, we have studied oscillatory instabilities of the nonlocal BSWs (Bragg solitary waves) and investigated collisions between them. It was demonstrated that nonlocal effect drastically stabilize the BSWs by reducing the growth rate of unstable eigenmodes of small perturbations, and that collisions between the solitons in the nonlocal setting can generate standing-light beams and pulses in a much broader range of the underlying parameter space than in the local medium. At the expense of the increased power, even solitons colliding at large velocities readily merge in the nonlocal medium. The effect of partial splitting of the merged beam into multiple transverse jets, which was also observed in the simulations, is realized as a manifestation of the nonlocality-induced spatial dispersion. The results indicate that Bragg solitons in nonlocal media have a potential for achieving the fundamental physical objective of the formation of standing-light pulses and beams, with feasible applications to all-optical data processing.

ACKNOWLEDGMENT

This work was supported by the National Science Council of Taiwan under Contract Nos. 95-2112-M-007-058-MY3 and NSC-95-2120-M-001-006.

[1] J. D. Joannopoulos, R. D. Meade, and J. N. Winn, *Photonic Crystals: Molding the Flow of Light* (Princeton University Press, Princeton, NJ, 1995), and reference therein.
[2] C. Lee, R. Radhakrishnan, C. Chen, J. Li, J. Thillaigovindan, and N. Balasubramanian, J. Lightwave Technol. **26**, 839 (2008).
[3] H. Kosaka, T. Kawashima, A. Tomita, M. Notomi, T. Tamamura, T. Sato, and S. Kawakami, J. Lightwave Technol. **17**, 2032 (1999).
[4] R. E. Slusher and E. J. Eggleton, *Nonlinear Photonic Crystals* (Springer, New York, 2003) and reference therein.
[5] M. Notomi, T. Tanabe, A. Shinya, E. Kuramochi, and H. Taniyama, Adv. Opt. Technol. **2008**, 568936 (2008) and references therein.
[6] D. N. Christodoulides and R. I. Joseph, Phys. Rev. Lett. **62**, 1746 (1989).
[7] A. Aceves and S. Wabnitz, Phys. Lett. A **141**, 37 (1989).
[8] B. J. Eggleton, R. E. Slusher, C. M. de Sterke, P. A. Krug, and J. E. Sipe, Phys. Rev. Lett. **76**, 1627 (1996); J. T. Mok, C. Martijn de Sterke, I. C. M. Littler, and B. J. Eggleton, Nat. Phys. **2**, 775 (2006).
[9] J. Feng, Opt. Lett. **18**, 1302 (1993).
[10] R. F. Nabiev, P. Yeh, and D. Botez, Opt. Lett. **18**, 1612 (1993).
[11] B. A. Malomed and R. S. Tasgal, Phys. Rev. E **49**, 5787 (1994).
[12] I. V. Barashenkov, D. E. Pelinovsky, and E. V. Zemlyanaya, Phys. Rev. Lett. **80**, 5117 (1998).
[13] A. A. Sukhorukov and Yu. S. Kivshar, Phys. Rev. E **65**, 036609 (2004).
[14] D. E. Pelinovsky, A. A. Sukhorukov, and Yu. S. Kivshar, Phys. Rev. E **70**, 036618 (2004).
[15] N. G. R. Broderick and C. M. de Sterke, Phys. Rev. E **55**, 3634 (1997).
[16] J. B. Khurgin, Phys. Rev. A **62**, 013821 (2000).

[17] P. J. Y. Louis, E. A. Ostrovskaya, and Y. S. Kivshar, Phys. Rev. A **71**, 023612 (2005).
[18] D. Janner, G. Galzerano, G. Della Valle, P. Laporta, S. Longhi, and M. Belmonte, Phys. Rev. E **72**, 056605 (2005).
[19] K. Yagasaki, I. M. Merhasin, B. A. Malomed, T. Wagenknecht, and A. R. Champneys, EPL **74**, 1006 (2006).
[20] T. Mayteevarunyoo and B. A. Malomed, Opt. Express **16**, 7767 (2008).
[21] K. Levy and B. A. Malomed, J. Opt. Soc. Am. B **25**, 302 (2008).
[22] H. Sakaguchi and B. A. Malomed, J. Phys. B **37**, 1443 (2004).
[23] W. C. K. Mak, B. A. Malomed, and R. L. Chu, Phys. Rev. E **68**, 026609 (2003).
[24] J. Atai, J. Opt. B: Quantum Semiclassical Opt. **6**, S177 (2004).
[25] D. Royston Neill, J. Atai, and B. A. Malomed, J. Opt. A, Pure Appl. Opt. **10**, 085105 (2008).
[26] J. E. Sipe, L. Poladian, and C. M. de Sterke, J. Opt. Soc. Am. A Opt. Image Sci. Vis **11**, 1307 (1994).
[27] W. C. K. Mak, B. A. Malomed, and P. L. Chu, J. Mod. Opt. **51**, 2141 (2004).
[28] J. T. Mok, C. M. de Sterke, and B. J. Eggleton, Opt. Express **14**, 11987 (2006).
[29] W. Królikowski, O. Bang, N. I. Nikolov, D. Neshev, J. Wyller, J. J. Rasmussen, and D. Edmundson, J. Opt. B: Quantum Semiclassical Opt. **6**, S288 (2004).
[30] Y. Y. Lin, R.-K. Lee, and Yu. S. Kivshar, J. Opt. Soc. Am. B **25**, 576 (2008).
[31] M. Peccianti, K. A. Brzdkiewicz, and G. Assanto, Opt. Lett. **27**, 1460 (2002).
[32] P. D. Rasmussen, O. Bang, and W. Królikowski, Phys. Rev. E **72**, 066611 (2005).
[33] Z. Xu, Y. V. Kartashov, and L. Torner, Phys. Rev. Lett. **95**, 113901 (2005).
[34] Y. Y. Lin, I. H. Chen, and R.-K. Lee, J. Opt. A, Pure Appl. Opt. **10**, 044017 (2008).
[35] B. A. Malomed, T. Mayteevarunyoo, E. A. Ostrovskaya, and Y. S. Kivshar, Phys. Rev. E **71**, 056616 (2005).
[36] I. V. Barashenkov and E. V. Zemlyanaya, Comput. Phys. Commun. **126**, 22 (2000).
[37] P. Günter and J.-P. Huignard, *Photorefractive Materials and Their Applications* (Springer Science, Berlin, 2006).
[38] C. C. Jeng, Y. Y. Lin, R.-C. Hong, and R.-K. Lee, Phys. Rev. Lett. **102**, 153905 (2009).
[39] K. Buse, Appl. Phys. B: Lasers Opt. **64**, 273 (1997).
[40] C. Conti, M. Peccianti, and G. Assanto, Phys. Rev. Lett. **92**, 113902 (2004).
[41] M. Peccianti, C. Conti, and G. Assanto, Phys. Rev. E **68**, 025602(R) (2003).
[42] D. Mihalache, D. Mazilu, F. Lederer, B. A. Malomed, Y. V. Kartashov, L. C. Crasovan, and L. Torner, Phys. Rev. E **73**, 025601(R) (2006).
[43] C. Rotschild, O. Cohen, O. Manela, M. Segev, and T. Carmon, Phys. Rev. Lett. **95**, 213904 (2005).
[44] R. Fischer, D. N. Neshev, W. Królikowski, Y. S. Kivshar, D. Iturbe-Castillo, S. Chavez-Cerda, M. R. Meneghetti, D. P. Caetano, and J. M. Hickman, Opt. Lett. **31**, 3010 (2006).
[45] V. Tikhonenko, J. Christou, and B. Luther-Davies, J. Opt. Soc. Am. B **12**, 2046 (1995).
[46] J. Schöllmann, Physica A **288**, 218 (2000).
[47] L. Allen and T. J. Bridges, Numer. Math. **92**, 197 (2002).
[48] G. Derks and G. A. Gottwald, SIAM J. Appl. Dyn. Syst. **4**, 140 (2005).
[49] T. Kapitula, N. Kutz, and B. Sandstede, Indiana Univ. Math. J. **53**, 1095 (2004).
[50] D. J. Kaup and T. I. Lakoba, J. Math. Phys. **37**, 308 (1996).
[51] D. J. Kaup and T. I. Lakoba, J. Math. Phys. **37**, 3442 (1996).
[52] R. S. Tasgal, Y. B. Band, and B. A. Malomed, Phys. Rev. Lett. **98**, 243902 (2007).
[53] B. J. Dabrowska, E. A. Ostrovskaya, and Y. S. Kivshar, J. Opt. B: Quantum Semiclassical Opt. **6**, 423 (2004).